A LASER INTERFEROMETRIC MINIATURE SEISMOMETER

Dustin W. Carr, Gregory R. Bogart, Seth Goodman, Patrick Baldwin, and David Robinson

Symphony Acoustics, Inc.

Sponsored by National Nuclear Security Administration

Contract Number DE-FG02-08ER85108

ABSTRACT

The threat of nuclear proliferation remains a critical issue in our society. Prevention requires knowledge, and there is no greater indicator of the capability and intent of a nation than observation of actual detonation tests being conducted. Ground-based monitoring systems have proven to be very capable in identifying nuclear tests, and can provide somewhat precise information on the location and yield of the explosive device. Making these measurements, however, currently requires very expensive and bulky seismometers that are difficult to deploy in places where they are most needed. A high-performance, compact device can enable rapid deployment of large scale arrays, which can in turn be used to provide higher quality data during times of critical need.

We are pursuing a design that is based upon a proven optical sensing modality, and will combine this interferometric transducer with a new mechanical system design in order to achieve the required sensor self-noise of 0.5 nano-g/$Hz^{1/2}$, with a total dynamic range of more than 150 dB. This will be accomplished in a form factor that is approximately 1 cm^3 per axis, and a power consumption below 30 mW. These metrics would represent substantial advancements over the existing state of the art.

Lower cost, smaller sensors will enable wide-scale deployment of sensor arrays, which will also greatly enhance our understanding of the earth and provide early-warning systems for earthquakes and tsunami. Slight variations in the sensor design will also find extensive use in oil and gas exploration.

Report Documentation Page

Form Approved
OMB No. 0704-0188

1. REPORT DATE	2. REPORT TYPE	3. DATES COVERED
SEP 2008		**00-00-2008 to 00-00-2008**

4. TITLE AND SUBTITLE	5a. CONTRACT NUMBER
A Laser Interferometric Miniature Seismometer	5b. GRANT NUMBER
	5c. PROGRAM ELEMENT NUMBER
6. AUTHOR(S)	5d. PROJECT NUMBER
	5e. TASK NUMBER
	5f. WORK UNIT NUMBER
7. PERFORMING ORGANIZATION NAME(S) AND ADDRESS(ES) **Symphony Acoustics Inc,103 Rio Rancho Blvd. NE,Rio Rancho,NM,87124**	8. PERFORMING ORGANIZATION REPORT NUMBER
9. SPONSORING/MONITORING AGENCY NAME(S) AND ADDRESS(ES)	10. SPONSOR/MONITOR'S ACRONYM(S)
	11. SPONSOR/MONITOR'S REPORT NUMBER(S)

12. DISTRIBUTION/AVAILABILITY STATEMENT
Approved for public release; distribution unlimited

13. SUPPLEMENTARY NOTES
Proceedings of the 30th Monitoring Research Review: Ground-Based Nuclear Explosion Monitoring Technologies, 23-25 Sep 2008, Portsmouth, VA sponsored by the National Nuclear Security Administration (NNSA) and the Air Force Research Laboratory (AFRL)

14. ABSTRACT
see report

15. SUBJECT TERMS

16. SECURITY CLASSIFICATION OF:			17. LIMITATION OF ABSTRACT	18. NUMBER OF PAGES	19a. NAME OF RESPONSIBLE PERSON
a. REPORT	b. ABSTRACT	c. THIS PAGE			
unclassified	**unclassified**	**unclassified**	**Same as Report (SAR)**	**9**	

OBJECTIVES

High-performance seismic sensors have seen little advancement over many years, and for good reason. It is very challenging to produce a compact, robust sensor with self-noise that approaches the low noise model (LNM) of earth motion. This noise floor is comparable to detecting the vibration from a snowflake landing nearby. The approaches that have been taken towards solving this problem have led to large sensor components. The smallest high-performance seismometers on the market that can approach the LNM are about the same size and weight as a bowling ball. Fundamental physical limits for an accelerometer, however, would indicate that much smaller devices are feasible.

We can achieve significant advancement in the state of the art by using a novel optical design that has been developed at Symphony Acoustics, Inc. for use in a variety of physical sensors. For a low frequency accelerometer, this optical design offers several advantages over comparable sensors that utilize electrostatic, magnetic, piezoelectric, or piezoresistive sensing:

- The sensing modality is decoupled from the proof-mass system.
- The sensing components are very small.
- The optical signal can be electrically chopped, thus eliminating issues with 1/f noise in the sensing electronics.

Our optical interferometric design leverages advancements in optical components, packaging, and miniaturization that have been driven by consumer electronics, optical storage, and optical communications markets. We employ an elegant design that utilizes a mixture of low cost materials and processes and commercial off-the-shelf (COTS) components. The design proposed herein can thus readily scale to volume manufacturing with a substantial cost advantage over any existing sensors.

Some of the earliest work describing these sorts of applications for interferometric transducers can be found in the patent literature, wherein generic forms of accelerometers and microphones have been proposed. Uda (1987) describes a Fabry-Perot transducer, while Haritonidis et al. (1990) describes a micromechanical Michelson interferometer. Work by Greywall (1999) looked at specific implementations using simple silicon-nitride designs and was the first to consider the possibility of placing all of the components in a small package. Transducers based on grating light valves developed by Solgaard et al. (1992) were explored by Lee et al. (2004) and Hall et al. (2005). Fabry-Perot based micro-electromechanical system (MEMS) accelerometers were fabricated and studied by Waters et al. (2002). Tunable Fresnel lens structures have been made with considerable success at SINTEF by Sagberg et al., (2003). Work by the principal investigator of the proposed work, Carr et al. (2003), studied a different type of lateral-motion grating. Follow-on work to this wherein the transducer was incorporated in an accelerometer with 17 ng/Hz$^{1/2}$ noise limit was provided by Krishnamoorthy et al. (2008).

This paper describes the proposed work for a new contract that has not yet begun. We will thus focus on the background information in this section, and conclude with a brief description of the work plan.

Fundamental Mechanical Considerations for Seismic Sensors

A seismic sensor is a device that detects ground motion by coupling the accelerations to an internal spring-mass system. Motion of the proof mass, *m*, is detected through a transducer that translates motion into an electrical voltage or current. In most, if not all, commercial devices, a feedback signal is fed into an actuator that holds the proof-mass in place, thus maintaining linearity and dynamic range. The discussion that follows herein is not entirely applicable to these closed-loop devices, because the dynamics of the feedback loop often dominate the considerations of both signal and noise. We are instead proposing a means for fabricating an open-loop freely moving proof mass system. Such an approach is enabled by the high dynamic range (150 dB) that is achievable with the optical detection system that we are proposing.

A good seismometer spring-mass system can be approximated very well as a linear device, with a Hooke's law spring constant *k*. This will have a fundamental mechanical resonance at a frequency of $\omega_0 = \sqrt{k/m}$. The resonant frequency is an important design parameter for two reasons. First, it is the transduction factor for converting an applied acceleration into a relative motion of the proof mass:

$$\Delta x = \frac{a}{\omega_0^{\,2}}. \tag{1.1}$$

Secondly, this frequency determines the bandwidth of the system. The exact useful bandwidth depends upon another parameter that measures the amount of mechanical damping in the system, which is the quality factor, or *Q*. For a system that is heavily underdamped, *Q*>>1, the operating bandwidth will typically extend from DC up to 1/3 to 1/2 of the resonant frequency, while an overdamped oscillator, *Q*<1, can have a bandwidth that extends up to the resonant frequency. These three parameters, mass, resonant frequency, and quality factor, determine all of the meaningful properties of the system, insofar as we neglect higher-order modes and cross-axis effects. We can now express the equation of motion in these terms

$$m\ddot{x} + m\frac{\omega_0}{Q}\dot{x} + m{\omega_0}^2 x = F_{ext} = ma_{ext}\,. \tag{1.2}$$

The second term is a mechanical resistance due to damping from any sources within the sensor system. This term is also responsible for thermal noise, just as resistance in an electrical circuit produces Johnson noise, as described by Gabrielson (1993). This is a white noise with a force spectral density given by

$$F_n = \sqrt{4k_B TR}\,(N/Hz^{1/2})\,, \tag{1.3}$$

wherein k_B is the Boltzmann constant and T is the temperature in Kelvin. By inspection of the equation of motion (1.2), we can see that the resistance is

$$R = \frac{m\omega_0}{Q}\,. \tag{1.4}$$

This noise force is applied directly to the proof mass, and thus results in an equivalent acceleration

$$a_n = \sqrt{\frac{4k_B T\omega_0}{mQ}}\,. \tag{1.5}$$

We will explore the magnitude of this noise source in combination with other noise sources in detail in the following section. As a point of reference, a system with a resonant frequency of 1 kHz, a mass of 1 gram, and a *Q* of 100, will have a thermal noise equivalent acceleration of about 3.2 ng/Hz$^{1/2}$, which is still 16 dB above the LNM.
The table below also gives some typical values for the amount of displacement in the proof mass when subjected to 1 g of acceleration.

Table 1. Typical values of proof-mass displacement when subjected to a 1g acceleration.

Resonant Frequency	Displacement at 1g
1 kHz	250 nm
100 Hz	25 μm
10 Hz	2.5 mm

If we take into account the thermal noise and the mechanical response, we can begin to understand why miniaturization and microelectromechanical systems (MEMS) technologies have had little impact to date upon low-noise seismometers. Silicon-based technologies are ill-suited for the problem. For a typical silicon wafer, with a thickness of 0.5 mm, the mass density is 0.13 grams/cm^2, which means that a significant fraction of a wafer would need to be consumed before we can approach even a mass of 1 gram. At the same time, if we reduce the frequency significantly below 1 kHz, we quickly run into very large displacements for micromechanical devices. This is why the best available accelerometers that utilize silicon MEMS remain 50 dB above the LNM.

Fundamental Optical Transducer Design Considerations

The basic operating principal involves the creation of an optical path whose length is varied when subjected to an external stimulus, such as pressure or acceleration. A Fabry-Perot type of interferometer can be used for consideration of the design issues in these types of transducers in general. This type of interferometer has two

parallel dielectric mirrors that bound an empty cavity as shown in Figure 1. Light that is incident upon the cavity will be partially transmitted according to the relation

$$T = \frac{1}{\left(1 + F \sin^2 \varphi/2\right)^2}, \tag{2.1}$$

wherein F is determined by the reflectance of the two mirrors,

$$F = \frac{4R_0}{\left(1 - R_0\right)^2}. \tag{2.2}$$

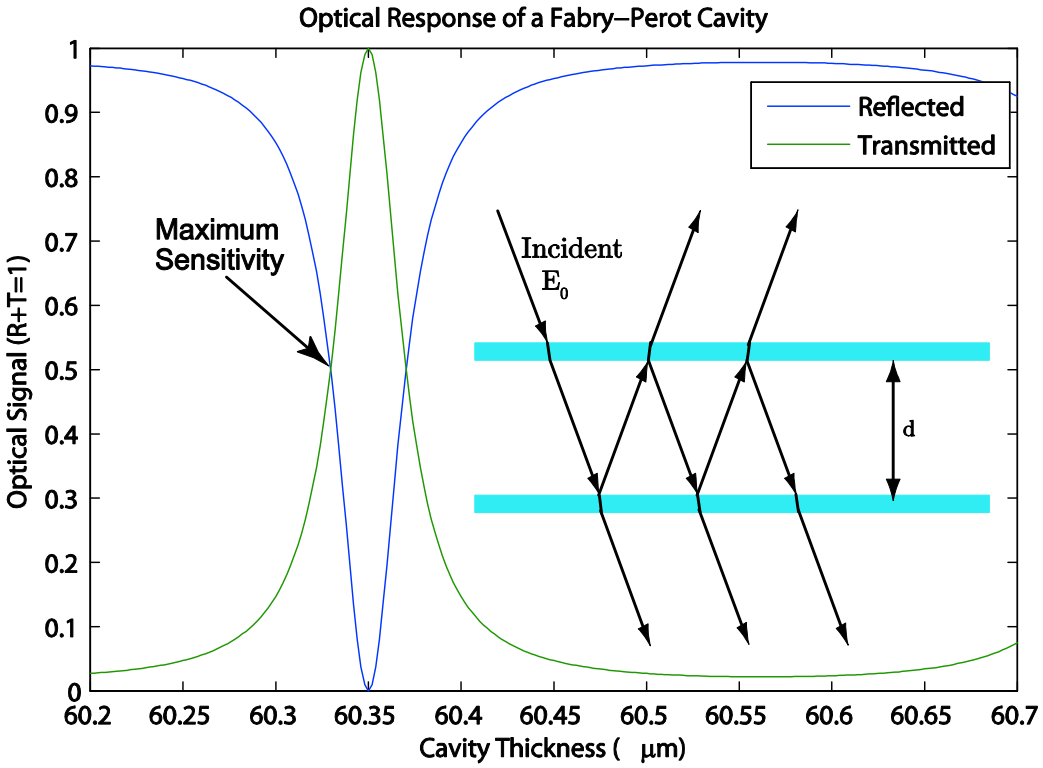

Figure 1. A planar Fabry-Perot device consists of two dielectric mirrors as shown in the inset. Multiple reflections within the cavity defined by the two mirrors can produce a resonant condition where maximum transmission is achieved. The reflected and transmitted light can be collected, and will display a maximum sensitivity to changes in the cavity thickness at the point indicated.

This assumes that the reflectance values of the two mirrors are equal. $\varphi = 4\pi d / \lambda$ is the phase that is picked up in a wave with wavelength λ as it makes a roundtrip within the cavity of length d. Figure 1 shows a typical response for a cavity whose mirrors have a moderate reflectance. From this plot, we see that the slope has a maximum value at the points indicated. The slope sensitivity of the transducer is the change in optical power at the detector-per-unit change in cavity length. The maximum slope can be shown to be

$$S_{\max} = \frac{I\pi}{\lambda}\sqrt{F - 1}\frac{W}{m}, \tag{2.3}$$

where I is the optical power.

From this we can start to see some of the potential benefit of the optical transducer. For illustration, a cavity with a reflectance of 0.7 on each side and an operating wavelength of 850 nm can achieve a relative sensitivity of 2%/nm. If we only consider laser relative intensity noise as the limit, we can still achieve a transducer noise floor that is below 1 pm/Hz$^{1/2}$, for a readily achievable intensity noise of -100 dB/Hz.

Theoretically, the true physical limit is going to be the photodiode shot noise. A differential detector can be designed that captures the reflected and transmitted signals, wherein the laser intensity noise is common to both and can thus be subtracted out, with the remaining noise limit being the photodiode shot noise.
The photodiode shot noise is given by the relation

$$n_{shot} = \sqrt{2eIB}\,\frac{A}{Hz^{1/2}}, \tag{2.4}$$

where e is the electron charge, I is the optical power that is incident upon the photodiode, and B is the photodiode sensitivity in units of Amperes/Watt.
Dividing this by the slope sensitivity in (2.3) and converting to acceleration using (1.1), we can arrive at an expression for the shot noise equivalent acceleration

$$h_{shot} = \frac{l\,w_0^{\,2}}{p}\sqrt{\frac{2e}{BI_0(F-1)}}\,\frac{m}{s^2 Hz^{1/2}}. \tag{2.5}$$

In practical designs, there are unfortunately additional sources of noise that are not necessarily common between the reflected and transmitted signals in a conventional Fabry-Perot design. In particular, shifts in the laser wavelength are going to produce a signal that is not discernible from a shift in the cavity length. This wavelength noise is going to depend upon the cavity length, and so a shorter cavity results in a lower impact on the effective noise. To be exact, if we have a known wavelength noise spectral density of $\delta\lambda$ in units of m/Hz$^{1/2}$, then this will result in an equivalent displacement noise of

$$\eta_\lambda = \delta\lambda\,\frac{d}{\lambda}\,\frac{m}{Hz^{1/2}}. \tag{2.6}$$

Other design considerations, however, prevent this cavity from becoming arbitrarily short. A practical range would be somewhere between 10 and 100 μm. In order to achieve a noise level that is equivalent to the shot-noise limit, this means that the laser wavelength must be maintained to better than 1 part in 10^9 per root Hz. While this is achievable in COTS diode lasers, it requires very careful design of the laser current control electronics. Given that the laser diodes have been optimized for applications that do not have this constraint, there is very little information on wavelength noise for COTS devices at the frequencies of interest for this application.

Note that laser wavelength noise is not related directly to the laser linewidth. The latter merely determines the coherence length of the laser, which is the distance that a wave packet can travel without the constituent waves falling out of phase. A shorter coherence length can result in a reduced signal amplitude in a transducer, but for cavity lengths around or below 100 μm, this is not a significant issue when quality laser diodes are utilized.

Because this source of noise typically has a strong 1/f component, it is very important to either reduce the wavelength noise through an active control technique, or somehow modify the design of the optical transducer such that it has less sensitivity to wavelength variation. Both of these approaches are being researched during this phase of the project.

Optical interference transducers have other mechanical advantages over their counterparts that use capacitive, piezoresistive, or piezoelectric sensing. First and foremost, the sensing mechanism is decoupled from the mechanical elements. Effectively, the motion of the structure being measured is “remote sensed.” An optical spot size that is as small as 10 μm can be used to interrogate the position. In other approaches, this is not typically the case. For instance, in a capacitively sensed device, the sensitivity will scale with the area of the electrodes, the distance between electrodes, and an applied voltage. The applied voltage in turn produces a force that must be accounted for in the design. All of these factors must be considered together in order to create an optimum design. In a

piezoelectric or piezoresistive device, appropriate materials must be used in the spring element, which is a significant manufacturing constraint.

The challenge in the optical design is that the response is only linear over a distance that is less than a quarter wavelength. There are many approaches for overcoming this limitation. The use of electrostatic actuators to compensate and pull the device to an optimum operating point has been proposed repeatedly. This approach introduces challenges that greatly reduce the potential benefits of the optical design when compared with other approaches. Introducing these actuators increases the complexity of the fabrication process, restricts the mechanical design space, and most importantly, creates a potential nightmare from a reliability standpoint. Laser wavelength can also be used as a control parameter, as a typical laser diode will have a wavelength that varies with the laser current. This is a more desirable design, as it allows the signal sensitivity to be directly controlled through the electronics. It does, however, require that the cavity length be sufficiently large (>50μm) (Figure 2).

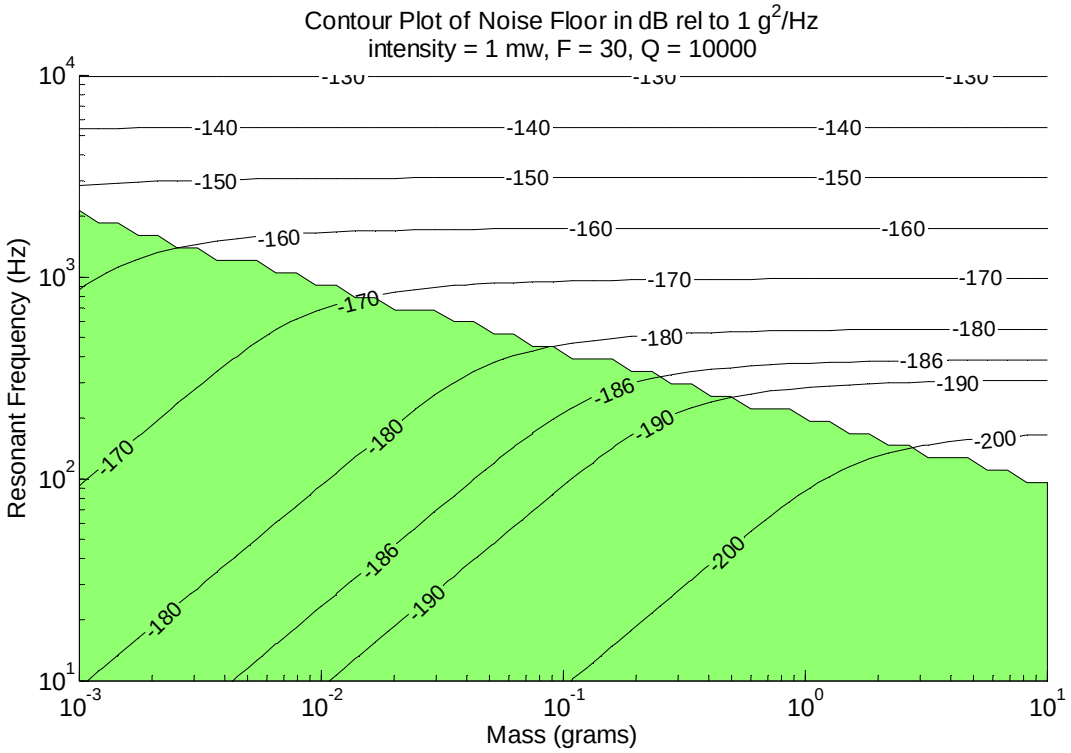

Figure 2. Contours of constant noise floor as a function of the key design parameters, resonant frequency and mass. The target level for the broadband white noise is -186 dB/Hz, or 0.5ng/Hz$^{1/2}$. Within the shaded region, the device is limited by thermal noise. Outside of this region, the limit is photodiode shot noise.

Electronics Design Considerations

Figure 3 is a block diagram of the electronics. There are a number of alternate topologies to produce an output corresponding to the difference between the two photodiode currents. Because the bandwidth of the system is relatively low and the dynamic range required is large, we choose to operate the photodiodes with zero bias, convert the photodiode currents to voltages with transimpedance amplifiers based on operational amplifiers (op amps) and produce a difference signal with a differential amplifier. Other approaches include a current proportioning differential transistor pair. The latter approach gives somewhat lower noise and automatically adjusts the relative gains of the two photocurrents to be equal, but it has potential linearity issues for this wide of a dynamic range.

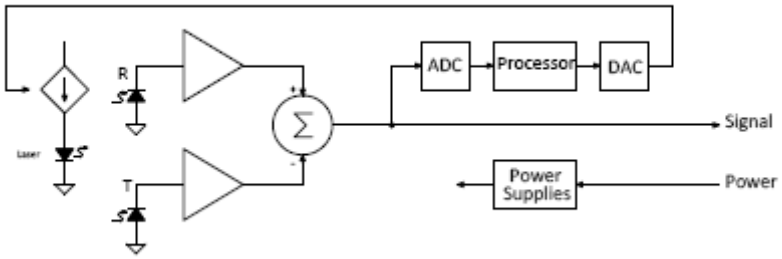

Figure 3. Block diagram of the electronics used for laser control and signal extraction. The laser current is controlled with a DAC voltage. The reflected and transmitted light is collected at the photodiodes and transimpedance amplifiers convert the photocurrent to a voltage, and the seismic signal is the difference between the two. An analog to digital converter uses the signal and the measured capsule temperature to apply corrections to the laser current.

We drive the Vertical Cavity Service Emitting Laser with a low-noise current source controlled by a microprocessor. Residual noise in the current source, plus intrinsic laser intensity noise, shows up as common to both photocurrents. These will cancel out to the extent that the total gain, optical plus electronic, is equal in the two signal paths. It is feasible to cancel the
laser-intensity noise far below the other noise sources without special measures.

Electronic noise in this system comes from a number of identifiable sources. All resistances have an associated thermal noise, or Johnson noise, which has a uniform (white) spectrum with voltage spectral density

$$V_n = \sqrt{4k_B TR}\,(V/Hz^{1/2}), \tag{3.1}$$

where V_n is voltage noise spectral density, k is Boltzman's constant, T is absolute temperature and R is resistance. Op amps have equivalent input voltage and current noise sources, which are both white, as well as 1/f noise components of both voltage and current. The 1/f components are especially important for accelerometers, as the frequency range extends far below the 1/f noise corners of most op amps.

Noise sources attributable to the opto-mechanical system are shot noise, determined by laser optical power output (2.4), and the thermal noise equivalent of the proof mass (1.5). Both of these sources are white. Each of these individual noise sources has a transfer function from their position in the circuit to the output which is, in general, a function of frequency. Thus, the total noise at the output of the circuit depends both on topology and component values. Total dynamic range depends not only on the noise floor, but also on the largest usable signal. To make best use of a particular topology, it is critical to scale the signal properly inside this usable range to the extent practical.

Figure 4 shows the output noise spectrum of a novel differential circuit developed in our facility and its two primary components. The "electronic" white noise level is roughly equal parts of op amp voltage noise and resistor thermal noise. The 1/f component is entirely op amp 1/f voltage noise. On the same figure, the opto-mechanical white noise is made up of the shot noise inherent in the 1mW optical beam power and the thermal equivalent mass noise of the proof mass. The electronic white noise level is apparently 13dB below the opto-mechanical white noise, so it makes a negligible contribution. Below the 8Hz 1/f noise corner, 1/f noise dominates and neither the electronic nor opto-mechanical white noise components contribute.

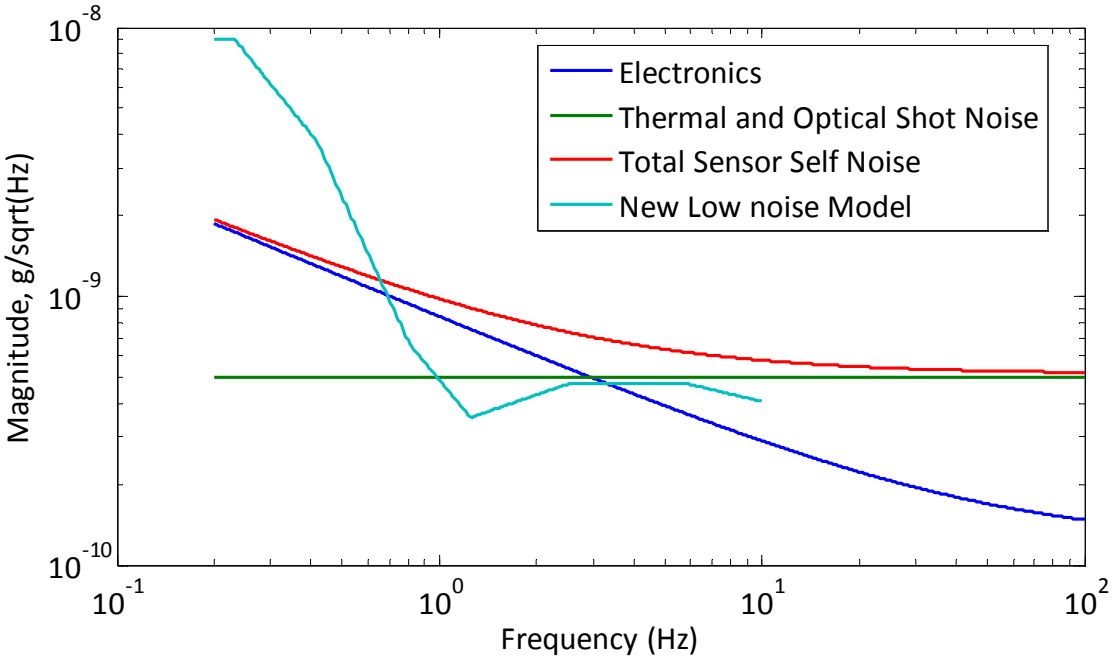

Figure 4. Predicted noise contributions using our existing electronics design. The 1/f components in the electronics produce noise that is in excess of the LNM target between 3 Hz and 0.8 Hz. Many solutions exist for overcoming this limitation. Chopping of the laser electronics, substituting lower noise operational amplifiers, or small changes in the circuit topology are all areas to be researched.

The proposed mechanical design has an acceleration scale factor that sets the high-frequency region of LNM at the same spectral level as opto-mechanical white noise. The LNM as described by Peterson (1993), with this scaling, is shown with the sum of electronic and opto-mechanical noise on Figure 4. This noise spectrum indicates that this initial design meets LNM everywhere except for the frequency range of 0.5-7Hz, where the 1/f noise dominates. The maximum signal size for this circuit is +5dBV, so the dynamic range is over 140dB.

For this topology, research work will involve reducing the 1/f noise power in the region where electronic noise is above LNM. Possible approaches are to modulate the signal out of the 1/f region by chopping the laser or by using chopper op amps. Other approaches are to create topology and/or component variations with noise spectra more suitable for the LNM. Increasing the light level by using a different laser, described in a previous section, also reduces electronic noise by decreasing the feedback resistance values in the transimpedance amplifiers.

CONCLUSIONS AND RECOMMENDATIONS

Achieving LNM resolution in a seismic sensor is a very strong challenge. While we have built sensors with noise performance below 100 ng/Hz$^{1/2}$, extending this to 0.5 ng/Hz$^{1/2}$ is not trivial. The research to be carried out in phase one will cover the following:

1. Development of a robust mechanical design that will result in a sufficient range of motion and a thermal noise limit that is below the LNM target, combined with an optical design that will result in the required motion sensitivity.
2. Characterization of optical sources to identify lasers that have sufficient power (up to 10 mW) and low enough wavelength noise, and identify methods to mitigate the effects of wavelength noise.
3. Development of an electronics design that will not contribute significantly to the noise floor defined by the photodiode shot noise and the mechanical thermal noise, and have an overall power consumption below 30 mW per axis.
4. Assembly and testing of a compact single axis sensor capsule that will demonstrate the feasibility of the approach. The assembly of functioning sensors components is critical in determining the overall feasibility of this approach. The multi-physical nature of this design demands that we not rely on laboratory bench

demonstrations, but actually make self-contained sensors, thus allowing us to fully uncover the critical details involved in the technical approach.

REFERENCES

Gabrielson, T. B. (1993). Mechanical-Thermal Noise in Micromachined Acoustics and Vibration Sensors. *IEEE Trans. Electron. Dev.* 40: pp. 903–909.

Uda, K. (1987). Pressure Sensitive Element. U.S. Pat. No. 4: 682,500

Haritonidis, J. H., S. D. Senturia, D. J. Warkentin, and M. Mehregany (1990). Optical Micropressure Transducer. U. S. Pat. No. 4,926,696

Greywall, D. S. (1999). Optical Interference Microphone. *Sens. Actuators.* 75: pp. 257–268.

Solgard, O. F.S.A. Sandejas, and D.M. Boom (1992). Deformable Grating Optical Modulator. *Opt. Lett.* 17: pp. 688–690,

Lee, W., N. A. Hall, Z. Zhou, and F. L. Degertekin (2004). Fabrication and Characterization of a Micromachined Acoustic Sensor With Integrated Optical Readout. *J. Sel. Topics. Quantum Electron.* 10: pp. 643–651,

Hall, N. A. B., Bicen, M. K. Jeelani, W. Lee, S. Qureshi, F. L. Degertekin, and M. Okandan (2005). Micromachined microphones with diffraction-based optical displacement detection. *J. Acoustical. Soc. Amer.* 118: pp. 3000–3009.

Waters, R. L and M. E. Aklufi (2002). Micromachined Fabry-Perot Interferometer for motion detection. *Appl. Phys. Let.* Vol. 81 pp. 3320–3322,

Sagberg, H., A. Sudbo, O. Solgaard, K.A.H. Bakke, and I.R. Johansen (2003). Optical Microphone Based on a Modulated Diffractive Lens. *IEEE Phot. Tech. Let.* 15: pp. 1431–1433,

Carr, D. W., J.P. Sullivan, and T.A. Friedmann (2003). Laterally Deformable nanomechanical zero-order gratings: Anomalous diffraction studied by rigorous coupled wave analysis. *Opt. Lett.* 28: pp. 1636–1638,

Keeler, B. E. N., D. W. Carr, J. P. Sullivan, T. A. Friedmann, and J. R. Wendt (2004). Experimental demonstration of a laterally deformable optical NEMS grating transducer. *Opt. Lett.* Vol. 29 pp. 1182–84.

Krishnamoorthy, U., D. W. Carr., G. R. Bogart, M. S. Baker, P. J. Clews, T. P. Swiler, and R. H. Olsson (2008). In-Plane MEMS-Based Nano-G Accelerometer with Sub-Wavelength Optical Resonant Sensor. *Sens. Act. A.* Vol. 145 pp. 283–290.

Peterson, J. (1993). Observations and Modeling of Seismic Background Noise. *OFR 93-322.*